Structural-acoustic model of a rectangular plate-cavity system with an attached distributed mass and internal sound source: Theory and Experiment

Miha Pirnat[a], Gregor Čepon[b], Miha Boltežar[b]

[a] KOLEKTOR ETRA d.o.o.,
Šlandrova ulica 10, 1231 Ljubljana-Črnuče, SI-Slovenia
[b] University of Ljubljana, Faculty of Mechanical Engineering,
Aškerčeva 6, 1000 Ljubljana, SI-Slovenia,
Fax: +386 1 2518-567,
Tel.: +386 1 4771-608,
E-mail: miha.boltezar@fs.uni-lj.si

Cite as:

Miha Pirnat, Gregor Čepon, Miha Boltežar, Structural-acoustic model of a rectangular plate-cavity system with an attached distributed mass and internal sound source: Theory and experiment, Journal of Sound and Vibration, Volume 333, Issue 7, 31 March 2014, Pages 2003-2018, ISSN 0022-460X, http://dx.doi.org/10.1016/j.jsv.2013.11.044.

Abstract:

In this paper three approaches are combined to develop a structural-acoustic model of a rectangular plate-cavity system with an attached distributed mass and internal sound source. The first approach results from a recently presented analysis based on the Raylegih-Ritz method and is used to circumvent the difficulties in obtaining the natural frequencies and mode shapes of a plate with an attached, distributed mass. Furthermore, different plate boundary conditions can be accommodated. The resulting mode shapes are defined as continuous functions; this is advantageous as they can be directly used in the second approach, i.e., the classic modal-interaction approach in order to obtain the coupled equations of the system. Finally, in the third approach a group of point sources emitting a pressure pulse in the time domain is used to model an internal sound source. For the validation of the developed model an experiment was conducted in two configurations using a simply supported aluminium plate and a clamped plate coupled with a plexiglas box containing a loudspeaker. Good agreement was found between the analytical and experimental data.

Keywords:

Plate-cavity system, Modal-interaction approach, Rayleigh-Ritz

---

1 Introduction

Analytical models based on a modal-interaction approach [1] can be used to represent a variety of structural-acoustic problems. They are frequently used to model enclosures with one flexible wall excited by an external sound field. Such plate-cavity systems provide a better insight into the physical principles than more complex systems analyzed with the finite-element method.

Some early investigations of plate-cavity systems were made by Dowell and Voss [2] and Lyon [3]. A general modal-interaction approach theory for the case of an external excitation is presented in [4] by Dowell et al. They also provide comparisons of the theory and experiment that show good agreement. More recently the coupled modal approach was used in the context of active noise cancelation. Al-Bassyiouni and Balachandran [5] used it for modeling the structural acoustics of sound transmission through a flexible panel into an enclosure. The panel was clamped along all four edges and the appropriate expressions for the mode-shape approximation were obtained from the work of Blevins [6]. Dupont et al. [7] used a plate-cavity system in the process of investigating the potential of active absorption for reducing low-frequency noise transmission out of an enclosure. A simply supported plate was used in the model and the experiment. Therefore, the analytical expressions were known for the plate mode shapes. For the excitation of the cavity a single point source located in the corner of the cavity was used. Venkatesham et al. [8] developed an analytical model for the calculation of beak-out noise from a rectangular plenum with four flexible walls. The latter were unfolded in order to obtain their mode shapes via the Rayleigh-Ritz approach. The inlet opening of the plenum was modeled as a piston source with uniform velocity.

Park et al. [9] proposed an analytical method for modeling the acoustic cavity coupled with a locally stiffened rectangular plate. This is modeled using a unique analytical method proposed by Yoon et al. [10]. The excitation of the simply supported plate is accomplished by the transverse loading of the plate and a point source in the interior.

A wide variety of means were used to battle the transmission of sound waves from the exterior to the interior of the plate-cavity system. The opposite case, when the wall is excited by an internal sound source, is rarely investigated. Additionally, the plate with an attached distributed mass coupled with an acoustic cavity represents a viable and often-used method for passive noise reduction.

It is known that the effects of a point mass can be used to reduce the radiated sound power from a structure. Pierre and Koopman [11] achieved large sound-power reductions by optimally placing strategically sized point masses on a plate. The mode shapes and the natural frequencies of the plate were obtained by using the finite-element method. Similarly, Constans et al. [12] used point masses on a cylindrical shell in order to minimize the radiated sound power. Using an optimization process in combination with the finite-element method a position of point masses on the shell was found that made the shell a weak radiator. Li and Li [13] studied the effects of the distributed masses on the acoustic radiation behavior of plates in air and water. A finite-element method was employed for the discretization of the structure and the Rayleigh integral was used for modeling the fluid.

It is clear that the application of a point mass can dramatically change the capability of a structure to radiate sound. However, a difficulty arises when one would like to study this effect on a plate-cavity system using a coupled modal approach. The uncoupled mode shapes of a mass-loaded plate must be known before a modal-interaction approach can be applied. The use of the finite-element method, as in references [11]-[13], is unsuitable as the results are given in discrete points and not as a continuous function. Additionally, the use of a single point source emitting in a limited frequency range as used by Dupont et al. [7] and Park et al. [9] is not sufficient when the coupled system is excited by a loudspeaker in the interior.

In this paper a structural-acoustic model of a plate-cavity system with an attached distributed mass and an internal sound source is developed by combining three approaches. First, a recently presented analysis with the Rayleigh-Ritz method [14] that is used to eliminate the difficulty of obtaining the '*in vacuo*' plate mode shapes and the natural frequencies of the plate with the attached distributed mass. In this way a wide range of plate boundary conditions can be easily accommodated. The appropriate approximation functions for different plate boundary conditions and the selection process for the key parameters are shown. Second, the modal-interaction approach is used to obtain the coupled equations of the system. Third, a group of sources representing a loudspeaker is used to emit a pressure pulse in the time domain. This ensures that all the frequencies are present in the excitation spectrum and not only a specified narrow band. To validate the developed structural-acoustic model an experiment is set up. A plexiglass box is coupled with two aluminium plates in two configurations and excited by an acoustic pulse from a loudspeaker in the interior. In first configuration all edges of the plate are simply supported and in the second configuration the edges are clamped. The structural and acoustic response is compared with the results from a computer implementation of the developed structural-acoustic model.

The article is organized as follows. First, a structural-acoustic model of the plate-cavity system is developed. Then an experimental setup is presented for the validation of the developed model. Finally, the analytical and experimental results are compared and discussed.

2 Structural-acoustic model

2.1 System description

The plate-cavity system considered in this paper consists of a flexible plate coupled with a rigid-wall acoustic cavity, see Fig.1. The plate can be clamped or simply supported along its edges in any combination. Additionally, it is loaded with a distributed mass of arbitrary dimensions $L_{\mathrm{dm},x}$ and $L_{\mathrm{dm},y}$ and a mass loading per unit area M. The system can be excited by a single point source or a group of point sources positioned at an arbitrary location in the cavity. In order to use the modal-interaction approach the uncoupled modal shapes and natural frequencies of the plate must be known '*a priori*'.

2.2 Obtaining the modal parameters of a plate loaded with a distributed mass

For the structural part of the modal-interaction approach the '*in vacuo*' normal modes and natural frequencies are needed. These are analytically

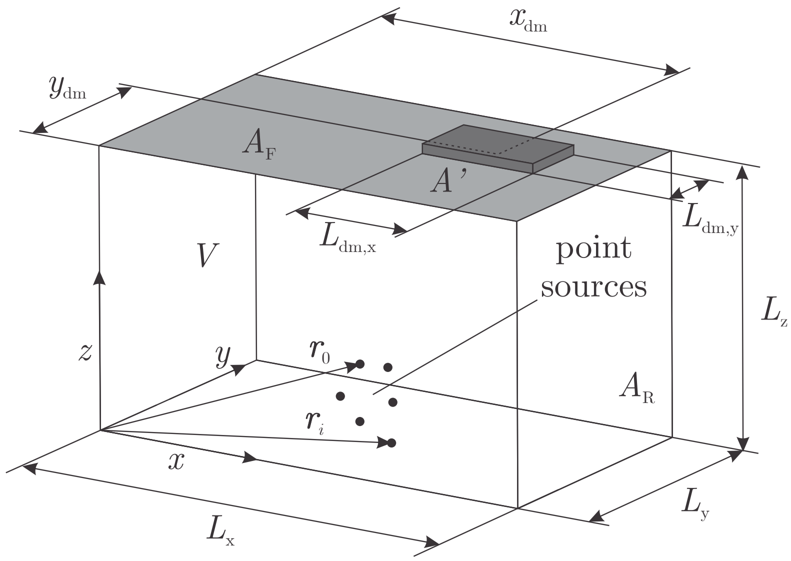

Figure 1: Scheme of the considered plate-cavity system.

known for the basic case of a simply supported plate without a distributed mass. However, when the distributed mass is attached, the plate modes and natural frequencies are no longer analytically obtainable. To circumvent this difficulty the results from a recently presented analysis of a mass-loaded plate based on the Rayleigh-Ritz approach [14] were used. The Rayleigh-Ritz method is suitable because the resulting mode shapes can be integrated as they are defined as continuous functions. Therefore, the results can be used directly in the modal-interaction approach.

If the effects of shear deformation and rotary inertia are neglected the dynamic equation for the deflection of a uniform isotropic rectangular plate with an attached distributed mass can be written as [14]:

$$\nabla^4 \left[\frac{Eh^3 w\left(x,y,t\right)}{12\left(1-\nu^2\right)} \right] + \frac{\partial^2 \left(\rho_{\mathrm{p}} h w\left(x,y,t\right)\right)}{\partial t^2} + \frac{\partial^2 \left(M A' w\left(x,y,t\right)\right)}{\partial t^2} = 0, \qquad (1)$$

where E is the Young's modulus, h is the thickness of the plate, w is the plate's normal displacement, ν is the Poisson ratio and ρ_{p} is the density of the plate material. Furthermore, t is the time, M is the distributed mass loading per unit area and A' is the area of the distributed mass. By assuming a simple harmonic vibration, the solution of equation (1) can be written as:

$$w\left(x,y,t\right)= \ W\left(x,y\right)\sin\left(\omega t\right), \tag{2}$$

where W represents the plate deflection shape at the angular frequency ω. If a modal approach is applied to equation (1) then $W(x,y)$ can be expressed as:

$$W\left(x,y\right)=\sum_{m}^{M}\sum_{n}^{N}W_{mn}\alpha_{m}\left(x\right)\beta_{n}\left(y\right), \tag{3}$$

where $\alpha_m\left(x\right)$ and $\beta_n\left(y\right)$ are the appropriate basis functions that individually satisfy at least the geometric boundary conditions in the x and y directions, respectively, and W_{mn} are unknown coefficients. The appropriate functions presented in Table 1 are from the work of Boay [15]. The coefficients W_{mn} are obtained by solving the generalized eigenvalue problem resulting from the Ritz method [14]:

$$\begin{aligned}
&\sum_{m}\sum_{n}\left\{C_{mnij}-\lambda\left[E_{mi}^{(0,0)}F_{nj}^{(0,0)}+\left(M/\rho_{\mathrm{p}}h\right)\hat{E}_{mi}^{(0,0)}\hat{F}_{nj}^{(0,0)}\right]\right\}W_{mn}=0,\\
&C_{mnij}=E_{mi}^{(2,2)}F_{nj}^{(0,0)}+E_{mi}^{(0,0)}F_{nj}^{(2,2)}+\nu\left(E_{mi}^{(0,2)}F_{nj}^{(2,0)}+E_{mi}^{(2,0)}F_{nj}^{(0,2)}\right)\\
&+2\left(1-\nu\right)E_{mi}^{(1,1)}F_{nj}^{(1,1)},
\end{aligned} \tag{4}$$

where the terms are defined as:

$$\begin{aligned}
E_{mi}^{(r,s)}&=\int_0^{L_{\mathrm{x}}}\left(\frac{\mathrm{d}^r\alpha_m}{\mathrm{d}x^r}\right)\left(\frac{\mathrm{d}^s\alpha_i}{\mathrm{d}x^s}\right)\mathrm{d}x, & F_{nj}^{(r,s)}&=\int_0^{L_{\mathrm{y}}}\left(\frac{\mathrm{d}^r\beta_n}{\mathrm{d}x^r}\right)\left(\frac{\mathrm{d}^s\beta_j}{\mathrm{d}x^s}\right)\mathrm{d}y,\\
\hat{E}_{mi}^{(r,s)}&=\int_{x_{\mathrm{dm}}-\frac{L_{\mathrm{dm,x}}}{2}}^{x_{\mathrm{dm}}+\frac{L_{\mathrm{dm,x}}}{2}}\left(\frac{\mathrm{d}^r\alpha_m}{\mathrm{d}x^r}\right)\left(\frac{\mathrm{d}^s\alpha_i}{\mathrm{d}x^s}\right)\mathrm{d}x, & \hat{F}_{nj}^{(r,s)}&=\int_{y_{\mathrm{dm}}-\frac{L_{\mathrm{dm,y}}}{2}}^{y_{\mathrm{dm}}+\frac{L_{\mathrm{dm,y}}}{2}}\left(\frac{\mathrm{d}^r\beta_n}{\mathrm{d}x^r}\right)\left(\frac{\mathrm{d}^s\beta_j}{\mathrm{d}x^s}\right)\mathrm{d}y,\\
\lambda&=\frac{\rho_{\mathrm{p}}h\omega^2}{D}, & D&=\frac{Eh^3}{12(1-\nu^2)},\\
&m,n,i,j=1,2,3..., & &r,s=0,1,2.
\end{aligned} \tag{5}$$

By using this approach it is also assumed that the attached distributed mass does not change the stiffness of the plate in any way. The selection process of the parameters M and N for a plate with all four edges simply supported (SSSS) or clamped (CCCC) is presented in Section 4.

Table 1: Appropriate functions to be used with different boundary conditions.

Two opposite edges	$\alpha_m(x)$	$\beta_n(y)$	
S-S	$\sin\left(\frac{m\,\pi\,x}{L_x}\right)$	$\sin\left(\frac{n\,\pi\,y}{L_y}\right)$	$m = 1, 2, 3, ...$ $n = 1, 2, 3, ...$
C-S	$\sin\left(\frac{\pi\,x}{2L_x}\right)\sin\left(\frac{m\,\pi\,x}{2L_x}\right)$	$\sin\left(\frac{\pi\,y}{2L_y}\right)\sin\left(\frac{n\,\pi\,y}{2L_y}\right)$	$m = 2, 4, 6, ...$ $n = 2, 4, 6, ...$
C-C	$\sin\left(\frac{\pi\,x}{L_x}\right)\sin\left(\frac{m\,\pi\,x}{L_x}\right)$	$\sin\left(\frac{\pi\,y}{L_y}\right)\sin\left(\frac{n\,\pi\,y}{L_y}\right)$	$m = 1, 2, 3, ...$ $n = 1, 2, 3, ...$

2.3 Modal-interaction approach

The Modal-interaction approach is best suited for weakly coupled systems. It is assumed that the plate-cavity system considered in this paper is weakly coupled (because cavity contains air) and therefore the modal-interaction approach can be applied. The governing differential equation of the acoustic cavity with the associated boundary conditions can be written (in terms of pressure) as [4]:

$$\nabla^2 p - \frac{1}{c^2}\frac{\partial^2 p}{\partial t^2} = 0, \tag{6}$$

$$\frac{\partial p}{\partial \boldsymbol{n}} = -\rho_{\mathrm{f}}\frac{\partial^2 w}{\partial t^2} \text{ on } A_{\mathrm{F}}, \tag{7}$$

$$\frac{\partial p}{\partial \boldsymbol{n}} = 0 \text{ on } A_{\mathrm{R}}, \tag{8}$$

where p is the internal acoustic pressure, ρ_{f} is the fluid density, c is the speed of sound and $\boldsymbol{n}$ is the normal vector. The rigid cavity walls are denoted by A_{R} and the surface of the flexible plate is denoted by A_{F}. Due to the boundary conditions (7) and (8) it is obvious that equation (6) will be coupled with equation (1) describing the plate vibration.

The governing differential equation of the plate with an attached mass coupled with an acoustic cavity can be written as:

$$\nabla^4\left[\frac{Eh^3 w\left(\boldsymbol{r}_{\mathrm{F}}, t\right)}{12\left(1-\nu^2\right)}\right] + \frac{\partial^2\left(\rho_{\mathrm{p}} h w\left(\boldsymbol{r}_{\mathrm{F}}, t\right)\right)}{\partial t^2} + \frac{\partial^2\left(M A' w\left(\boldsymbol{r}_{\mathrm{F}}, t\right)\right)}{\partial t^2} = p^{\mathrm{c}}\left(\boldsymbol{r}_{\mathrm{F}}\right) + p^{\mathrm{E}}\left(\boldsymbol{r}_{\mathrm{F}}\right), \tag{9}$$

where vector $\boldsymbol{r}_{\mathrm{F}}$ corresponds to the plate surface A_{F}, p^{c} is the pressure loading due to the cavity acoustics and p^{E} due to some external element. Equation (9) can be condensed to read:

$$\nabla^4 \left[\frac{Eh^3 w\left(\boldsymbol{r}_{\mathrm{F}}, t\right)}{12\left(1-\nu^2\right)} \right] + m\left(\boldsymbol{r}_{\mathrm{F}}\right) \frac{\partial^2 w\left(\boldsymbol{r}_{\mathrm{F}}, t\right)}{\partial t^2} = p^{\mathrm{c}}\left(\boldsymbol{r}_{\mathrm{F}}\right) + p^{\mathrm{E}}\left(\boldsymbol{r}_{\mathrm{F}}\right), \tag{10}$$

where m denotes the plate mass per unit area and incorporates the effect of the attached mass. Expanding equations (6) and (10) in terms of the uncoupled normal modes yields the modal-interaction equations of motion with included viscous damping terms [1]:

$$\begin{aligned} &\ddot{W}_p(t) + 2\varsigma_p \omega_p \dot{W}_p(t) + \omega_p^2 W_p(t) = \\ &\frac{1}{\Lambda_p} \int\limits_{A_{\mathrm{F}}} p^{\mathrm{E}}\left(\boldsymbol{r}_{\mathrm{F}}\right) \Phi_p\left(\boldsymbol{r}_{\mathrm{F}}\right) \mathrm{d}S + \frac{1}{\Lambda_p} \sum_{n=1}^{\infty} p_n(t) \int\limits_{A_{\mathrm{F}}} \Psi_n\left(\boldsymbol{r}_{\mathrm{F}}\right) \Phi_p\left(\boldsymbol{r}_{\mathrm{F}}\right) \mathrm{d}S \end{aligned} \tag{11}$$

and for the fluid:

$$\begin{aligned} &\ddot{p}_n(t) + 2\varsigma_n \omega_n \dot{p}_n(t) + \omega_n^2 p_n(t) = \\ &-\frac{\rho_{\mathrm{f}} c^2}{V} \sum_{p=1}^{\infty} \ddot{W}_p(t) \int\limits_{A_{\mathrm{F}}} \Psi_n\left(\boldsymbol{r}_{\mathrm{F}}\right) \Phi_p\left(\boldsymbol{r}_{\mathrm{F}}\right) \mathrm{d}S + \frac{\rho_{\mathrm{f}} c^2}{V} \int\limits_{V} \frac{\partial q(\boldsymbol{r})}{\partial t} \Psi_n(\boldsymbol{r}) \mathrm{d}V, \end{aligned} \tag{12}$$

where the term Λ_p is defined as $\int\limits_{A_{\mathrm{F}}} m\left(\boldsymbol{r}_{\mathrm{F}}\right) \Phi_p^2\left(\boldsymbol{r}_{\mathrm{F}}\right) \mathrm{d}S$. The first term on the right-hand side of equation (11) represents some external loading of the plate and the second term is the contribution due to the coupling with the acoustic pressure. The first and second terms on the right-hand side of equation (12) represent the contributions due to the coupling with the plate and due to the interior sound source, respectively, where q denotes source volume velocity per unit volume. From equations (11) and (12) it is also clear that a single acoustic mode excites an infinite number of structural modes and vice versa.

The expansions used in the derivation of equations (11) and (12) are:

$$p(\boldsymbol{r}, t) = \sum_{n=0}^{\infty} p_n(t)\, \Psi_n(\boldsymbol{r}) \tag{13}$$

and

$$w\left(\boldsymbol{r}_{\mathrm{F}}, t\right)=\sum_{p=1}^{\infty} W_{p}\left(t\right) \Phi_{p}\left(\boldsymbol{r}_{\mathrm{F}}\right), \tag{14}$$

where p_n is the n-th modal pressure amplitude, Ψ_n is the n-th acoustic cavity rigid-wall mode shape, W_p is the p-th modal displacement amplitude and Φ_p is the p-th uncoupled plate mode shape obtained with the Rayleigh-Ritz method in the previous section.

2.4 Implementation of the internal sources

In order to excite the plate-cavity system, a pressure pulse is introduced in the time domain. This excites all the system modes uniformly across the frequency spectrum.

If a delta function is introduced into the source term in equation (12) the integration is effectively limited to a point-source location $\boldsymbol{r}_0$:

$$\frac{\rho_{\mathrm{f}}\, c^{2}}{V} \int_{V} \frac{\partial q\left(\boldsymbol{r}\right)}{\partial t} \delta\left(\boldsymbol{r}-\boldsymbol{r}_{0}\right) \Psi_{n}\left(\boldsymbol{r}\right) \mathrm{d} V. \tag{15}$$

Assuming that q is independent of $\boldsymbol{r}$ the result of the integration is:

$$\frac{\rho_{\mathrm{f}}\, c^{2}}{V} \dot{q}_{0}\, \Psi_{n}\left(\boldsymbol{r}_{0}\right). \tag{16}$$

By choosing:

$$q_{0}=A_{0} \sin\left(\omega_{0} t\right), \tag{17}$$

the term (16) changes to:

$$\frac{\rho_{\mathrm{f}}\, c^{2} A_{0} \omega_{0}}{V} \cos\left(\omega_{0} t\right) \Psi_{n}\left(\boldsymbol{r}_{0}\right), \tag{18}$$

which represents the effect on the n-th acoustic mode by a single source located at point $\boldsymbol{r}_0$, pulsating with the angular frequency ω_0 and amplitude A_0. In order to represent a group of sources emitting a pressure pulse in the time domain, the term (18) is expanded to read:

$$\frac{\rho_{\mathrm{f}}\, c^{2}}{V} \sum_{n}^{\infty} \sum_{i}^{N_{\mathrm{S}}} \sum_{j}^{\infty} A_{ij} \omega_{j} \cos\left(\omega_{j} t\right) \Psi_{n}\left(\boldsymbol{r}_{i}\right), \tag{19}$$

where N_S is the number of sources.

By using the appropriate frequency components the term (19) can be used to represent not only the pressure pulse but also any other harmonic excitation.

3 Experiment

In order to verify the presented structural-acoustic model an experiment was set up as shown in Fig. 2. A parallelepiped plexiglas box was constructed using 30-mm-thick panels. The cavity of the box has the following dimensions: $L_x = 0.78$ m, $L_y = 0.45$ m and $L_z = 0.47$ m, see Fig. 3 and Table 2. The top of the box was covered by two different plates to accommodate the simply supported and clamped boundary condition. A 3-mm-thick aluminium plate was simply supported by using a steel frame and a special 0.2-mm-thick adapter, as shown in Fig.4(a). For the clamped boundary condition a 1.5-mm-thick aluminum plate was placed directly between the steel frames, as shown in Fig. 4(b). To ensure an air-tight seal an O-ring gasket was inserted between the frame and the box. A loudspeaker was positioned in the corner of the cavity. In this way all the acoustic modes of interest could be appropriately excited.

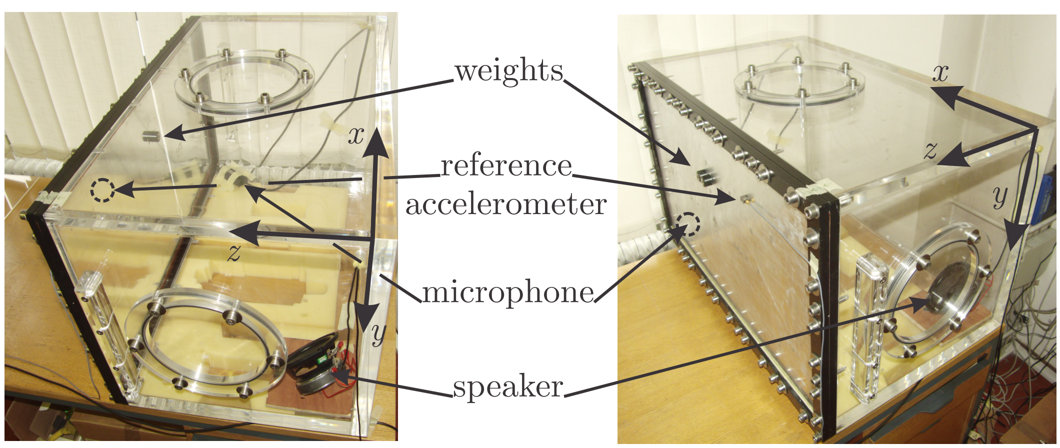

Figure 2: Experimental plate-cavity system.

The measurement chain used in the experiment is presented in Fig. 5. The acoustic-cavity pressure response was measured at point $\boldsymbol{r}_{\mathrm{Mic}}$ using a PCB 378B02 microphone. Additionally, a Polytec PDV-100 laser vibrometer

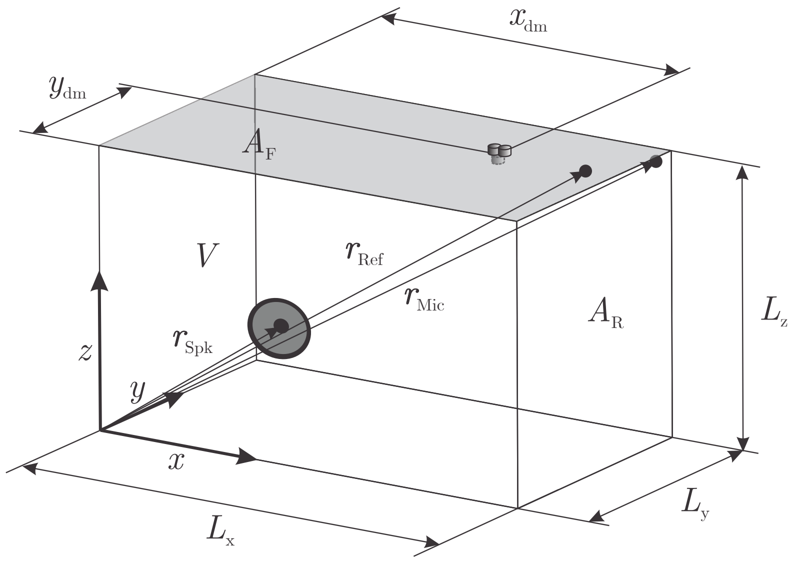

Figure 3: Scheme of the experimental plate-cavity system.

Table 2: Locations of the microphone, the reference accelerometer and the loudspeaker.

	x [m]	y [m]	z [m]
$\boldsymbol{r}_{\mathrm{Mic}}$	0.765	0.435	0.455
$\boldsymbol{r}_{\mathrm{Ref}}$	0.2	0.08	0.47
$\boldsymbol{r}_{\mathrm{Spk}}$	0.07	0.362	0.08

was used to measure the plate velocity on a rectangular grid of measurement points consisting of 15 rows and 25 columns. A computer-controlled table was used to successively target the laser at each of the 375 measurement points. An additional measurement point $\boldsymbol{r}_{\mathrm{Ref}}$ was used as a phase reference during the assembly of the plate-velocity data into mode shapes.

In the experiment a square wave with a duty cycle of a 0.00625% was generated and fed to a Bellesound Pro4800 laboratory power amplifier. In order to generate an acoustic pulse the amplified signal drove a Monacor SPH-135 AD loudspeaker with a 39 Hz to 6 kHz usable frequency range and a membrane radius of $r_{\mathrm{s}} = 0.05\,\mathrm{m}$. The center of the loudspeaker membrane was located in a corner at $\boldsymbol{r}_{\mathrm{Spk}}$ and was rotated in such a position that the plane of the membrane cut the surrounding three walls at a 45° angle.

During the experiment the data was sampled using a 25.6 kHz sampling frequency over a 2 s time period, which defined the frequency resolution as 0.5 Hz. To acquire the velocity data at a grid point an acoustic pulse was generated and at the same time the 2 s data acquisition began. Then the system was left to reach a static, stationary state before the next measurement was started. In order to reduce the noise in the measurement data, the velocity measurements were averaged in the frequency domain. A similar procedure was employed when acquiring the pressure data. Additionally, all the necessary measurements were completed in rapid succession in order to keep the effect of changing the ambient temperature at a minimum.

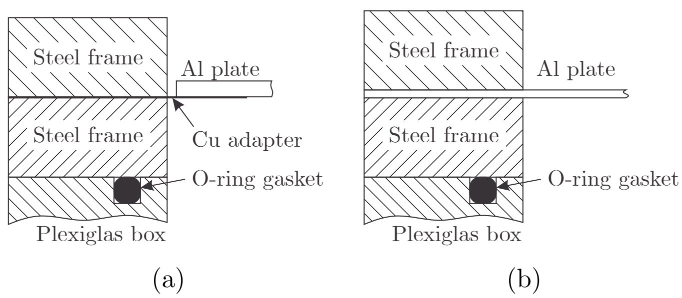

Figure 4: Implementation of different boundary conditions in the experiment; (a) Simply supported boundary conditions, (b) Clamped boundary conditions.

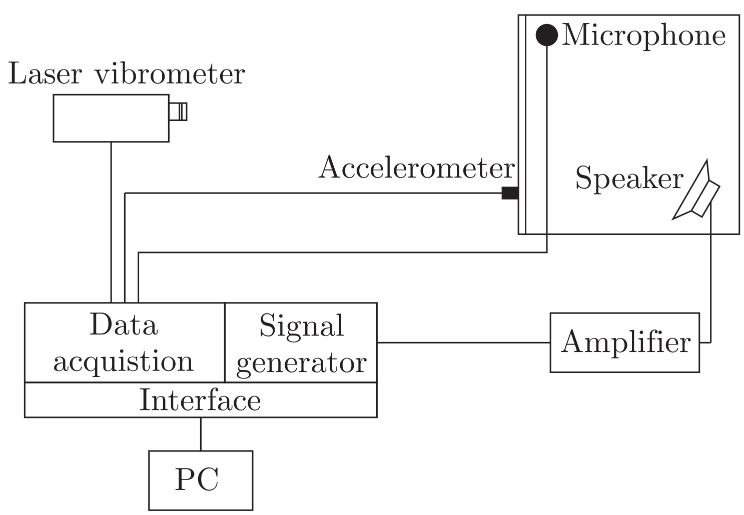

Figure 5: The measurement chain used in the experiment.

To provide the data for the model validation, two different load cases were used for each plate boundary condition, see Table 3. To implement the load cases a maximum of three identical cylindrical weights were used, each with a diameter of 0.025 m, a height of 0.016 m and a weight of approximately 50 g. When all three weights were used, one was positioned on the interior side of the plate and the other two on the exterior, as shown on Fig. 3. The parameters x_{dm} and y_{dm} in Table 3 represent the approximate location of the center of gravity of the attached masses. As the purpose of this paper is not optimization of the parameters x_{dm} and y_{dm}, but validation of the presented structural-acoustic model, the parameters x_{dm} and y_{dm} were chosen arbitrarily. This is reasonable due to the fact that the plate dynamics and thus response of the coupled system, is affected for any location of the added mass.

Table 3: Experiment load cases.

Load case	LC-1S	LC-2S	LC-1C	LC-2C
Boundary cond.	SSSS	SSSS	CCCC	CCCC
Mass [g]	0	150	0	50
$x_{\mathrm{dm}}[m]$	/	0.39	/	0.135
$y_{\mathrm{dm}}[m]$	/	0.11	/	0.36

For each of the load cases a pressure response was measured using the microphone positioned at point $\boldsymbol{r}_{\mathrm{Mic}}$. To obtain the plate mode shapes an operational deflection shape (ODS [16]) analysis was used. An ODS can be defined as the deflection of a structure at a particular frequency, hence only the response measurements are needed for the analysis. However, an additional phase reference is needed for the synchronization of multiple response measurements. In this work a laser vibrometer was used to measure the plate velocity on a rectangular grid consisting of 375 measurement points. The plate-velocity data was synchronized using phase data from the reference accelerometer. The number of velocity-field measurement points provides a smooth representation of the simply-supported plate modes up to 550 Hz and clamped plate modes up to 320 Hz. Based on this and the used measurement equipment the useable frequency range of the data is between 45 Hz and 550 Hz for the simply supported plate and between 45 Hz and 320 Hz for the clamped plate. The pressure amplitude spectrum and the RMS amplitude spectrum of the plate-displacement field will be used together with the mode shapes to validate the structural-acoustics model in the subsequent sections.

4 Implementation of the structural-acoustic model

To obtain the analytical results the described structural-acoustic model was implemented in the Python computer language. The dimensions of the cavity and the plate are considered to be the same as those used in the experiment. Also, the loudspeaker location and the pressure sampling point are at the same location as in the experiment, see Fig. 3. Additionally, the exterior pressure loading of the plate p^{E} in equation (11) is assumed to be much smaller than p^{c}, i.e. $p^{E} = 0$. This assumption is valid as the sound source is located in the interior of the cavity and no additional sound sources are present in the exterior.

To model the simply supported and clamped plate using the Rayleigh-Ritz approach the appropriate functions from Table 1 were used. In order to correctly select the parameters M and N in equation (3) an error analysis was made. A finite-element method (FEM) was used to obtain a set of natural frequencies for the simply supported and clamped plate. Then a relative error can be defined for the i-th plate natural frequency between the FEM results and the Rayleigh-Ritz results as:

$$err_i = \frac{f_{\mathrm{RR},i} - f_{\mathrm{FEM},i}}{f_{\mathrm{FEM},i}} \cdot 100. \tag{20}$$

However, a structural-acoustic model consists of several structural modes. Therefore, a measure of the error for the first 20 plate modes is calculated using a root-mean-square approach:

$$err_{\mathrm{RMS}} = \sqrt{\frac{\sum_{i=1}^{20} err_i^2}{20}}. \tag{21}$$

Using equation (21) the err_{RMS} was calculated for a large selection of parameters M and N with the only limitation being that $M \cdot N \geq 20$. In Table 4 a sample of results is presented, showing the lowest obtained errors. It is clear that for the simply supported plate the optimal selection of parameters is $M = 7$ and $N = 4$ and for clamped plate $M = 14$ and $N = 7$. A significantly larger number of terms is needed for the clamped plate; however, the ratio M/N is similar for both boundary conditions and is close to the ratio L_x/L_y.

Table 4: RMS of relative error between FEM and Rayleigh-Ritz results for different M and N.

Simply supported plate			Clamped plate		
M	N	err_{RMS} [%]	M	N	err_{RMS} [%]
6	4	1.987	13	6	0.375
6	5	1.987	13	7	0.219
6	6	1.987	13	8	0.245
7	3	5.889	14	6	0.362
7	4	0.351	14	7	0.212
7	5	0.351	14	8	0.249
8	3	5.889	15	6	0.356
8	4	0.351	15	7	0.220
8	5	0.351	15	8	0.260

The definition of the load cases for the analytical model presented in Table 5 gains an additional two parameters in order to fully describe the distributed mass. The parameters $L_{\mathrm{dm},x}$ and $L_{\mathrm{dm},y}$ were chosen so that A' approximated the plate area to which the weights were attached.

Table 5: Additional parameters for the definition of the load cases.

	LC-1S	LC-2S	LC-1C	LC-2C
$L_{\mathrm{dm},x}[m]$	/	0.05	/	0.025
$L_{\mathrm{dm},y}[m]$	/	0.025	/	0.025

A group of ten point sources was used to represent the loudspeaker used in the experiment. The sources were distributed on two parallel planes $t_{\mathrm{s}} = 0.03\,\mathrm{m}$ apart in a circular order, as shown in Fig. 6. The sources in the $y'z'$ plane had a positive amplitude and the others had a negative amplitude. The formulation described in Section 2.4 was used to model the impulse excitation of the loudspeaker.

To solve the coupled set of differential equations (11) and (12) some trivial initial conditions were used. The model consisted of twenty-two uncoupled acoustic modes and eighteen uncoupled plate modes, which are for different load cases presented in Tables 6 and 7, respectively. The number of modes taken into consideration covers a frequency range which is wider than that of the experiment. This is necessary as some higher acoustic modes have a significant effect on the coupled system's response, even in the low-frequency

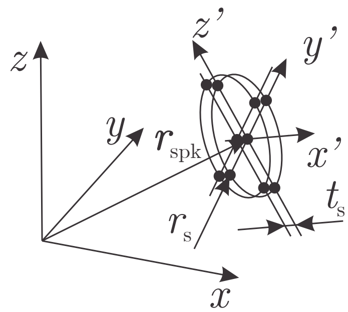

Figure 6: Point-source representation of the loudspeaker.

range.

Table 6: First ten uncoupled acoustic-cavity modes and acoustic damping factors used in the model for all load cases.

Mode	Natural Freq. [Hz]	Damping[a] [/]	
		Simply supported b.c.	Clamped b.c.
1	0	/	/
2	220	0.001	0.0015
3	365	0.0013	0.0015
4	381	0.0008	0.0015
5	426	0.003	0.0005
6	440	0.0008	0.0005
7	440	0.0023	0.0005
8	528	0.002	0.0005
9	572	0.0001	0.0005
10	572	0.0001	0.0005

[a]: Based on comparison between measured data and results from the model.

The structural and acoustic modal damping parameters used in equations (11) and (12) are shown in Tables 6 and 7. Their values were obtained by comparing the measured data with results from structural-acoustic model for load cases LC-1S and LC-1C. It is assumed that the damping does not change due to attached mass.

The resulting time-domain modal pressures and displacement amplitudes were casted into the frequency domain with 0.5 Hz resolution using a Fourier transformation. Then the pressure-amplitude spectrum at the point $\boldsymbol{r}_{\rm Mic}$ could be calculated. Furthermore, the plate displacements were calculated

Table 7: Uncoupled plate modes and structural damping factors used in the model for LC-1S and LC-1C.

Mode	Simply supported b.c.		Clamped b.c.	
	Natural freq.[a] [Hz]	Damping[b] [/]	Natural freq.[a] [Hz]	Damping[b] [/]
1	48.5	0.009	45.4	0.004
2	84.6	0.008	64.2	0.003
3	144.8	0.01	97	0.005
4	157.6	0.01	115	0.023
5	193.7	0.005	133	0.0045
6	229.2	0.006	143	0.01
7	254	0.001	163.9	0.01
8	337.7	0.01	202.1	0.007
9	338.4	0.04	207.8	0.025
10	339.5	0.005	220.6	0.005
11	375.7	0.02	238.5	0.008
12	436	0.008	265.3	0.012
13	446.8	0.01	268.9	0.008
14	470.2	0.01	273.3	0.017
15	520.3	0.04	311.8	0.01
16	579.4	0.01	335	0.001
17	594.2	0.001	358.3	0.001
18	627	0.001	361.3	0.001

[a]: Obtained with the Rayleigh-Ritz method.

[b]: Based on comparison between measured data and results from the model.

at the same grid points as used in the experiment. Finally, a fine grid was used in order to generate accurate mode shapes for a comparison with the experiment.

5 Results and discussion

In this section the analytical and experimental results are compared in order to validate the presented structural-acoustic model. The comparison was made using the sound pressure level at the point $\boldsymbol{r}_{\text{Mic}}$, the plate mode shapes and the RMS plate-displacement level based on all 375 grid points. The correlation between the calculated and the measured plate-mode shapes was established using a modal assurance criterion (MAC) [17]. Additionally, in Table 8 an overview of the mode frequencies for all the load cases is presented. The results show an average relative error of approximately 1% between the analytical and experimental data and are considered to be in a good agreement.

Table 8: Experimental and analytical mode frequencies of the coupled system for all the load cases.

	LC-1S		LC-2S		LC-1C		LC-2C	
Mode	Ana. [Hz]	Exp. [Hz]	Ana. [Hz]	Exp. [Hz]	Ana. [Hz]	Exp. [Hz]	Ana. [Hz]	Exp. [Hz]
1	54	50.5	52	48	48	51.5	48	52
2	84	81.5	84	81.5	64	63	63.5	63.5
3	144.5	143	132	130	97	97	94	97
4	157	153.5	150	147.5	115	111	112	110.5
5	193	192	192	191	133	130.5	124	126.5
6	219	219.5	219	219	143	141.5	139.5	141.5
7	231	230	230	229.5	164	160.5	155	155
8	253.5	256	236	238	202	200	191	191
9	337	335	319	315	207	204	203.5	203.5
10	370	369	337.5	332	220	220.5	220	220
11	375	372	369	369	239	237	230	230
12	382	384	374	372	269	264	253	250
13	428	429	382	384	273	271	266	265
14	434	436	415	415	312	306	272.5	272.5
15	442.5	444	428	429			301	297.5
16	446.5	453	438	441				
17	470.5	466	443	445				
18	520	527	464	462				
19	529	531	516	524.5				
20			529	531				
Avg.^{a}		1.20		1.41		1.33		0.96

^{a}: Average relative error in %.

5.1 Simply-supported plate

In Fig. 7 the RMS plate-displacement spectra are shown for the simply supported plate. The effect of the attached mass is most noticeable at 250

Hz and 340 Hz. The plate-controlled modes shift to the left due to the added mass. The first cavity-controlled mode at 220 Hz and the 230 Hz mode are unaffected as the mass is in the node of the mode dominating response in that region. The added mass changes the mode shape of the second cavity-controlled mode at 370 Hz, as shown in Fig. 8; however, its amplitude and frequency are unaffected. The effects of the added mass can also be seen in the sound pressure level spectra presented in Fig. 9. Additionally, it can be seen that the cavity-controlled modes at 440 Hz are also significantly affected. It is clear that the structural-acoustic model correctly predicts the changes of the plate and cavity-controlled modes due to added mass.

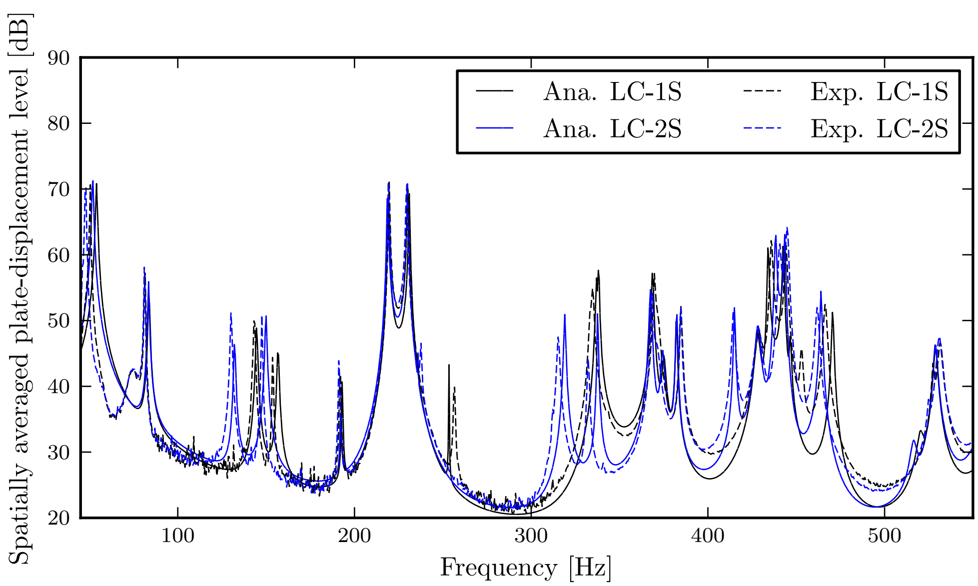

Figure 7: RMS plate-displacement level spectrum for LC-1S and LC-2S.

5.2 Clamped plate

In Fig. 10 the RMS plate-displacement spectra are shown for the clamped plate. Most notable changes are in the frequency range from 180 Hz to 260 Hz. The plate-controlled modes shift to the left due to the added mass. The amplitude and frequency of the cavity-controlled mode at 220 Hz are again unaffected. However, the added mass changes its mode shape as shown in 11. The effects of the added mass can also be observed in Fig. 12. It can be

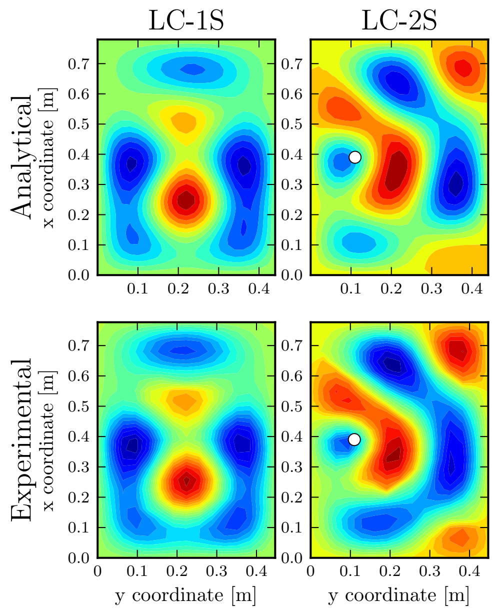

Figure 8: Comparison of the simply-supported plate mode shapes at second cavity controlled mode at approximately 370 Hz. The symbol '○' represents the mass location.

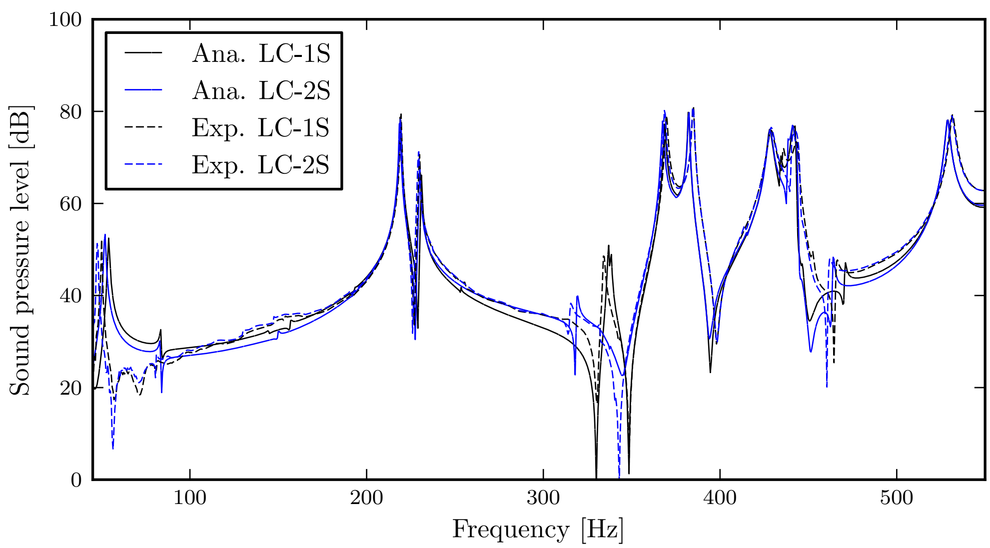

Figure 9: Amplitude spectrum of sound-pressure level for LC-1S and LC-2S.

seen that the overall agreement is good, although some discrepancies exist in the amplitudes between the analytical and experimental data. This is due to the fact that the clamped boundary conditions are difficult to replicate in the experiment and that the clamped plate's natural frequencies are very sensitive to ambient temperature changes.

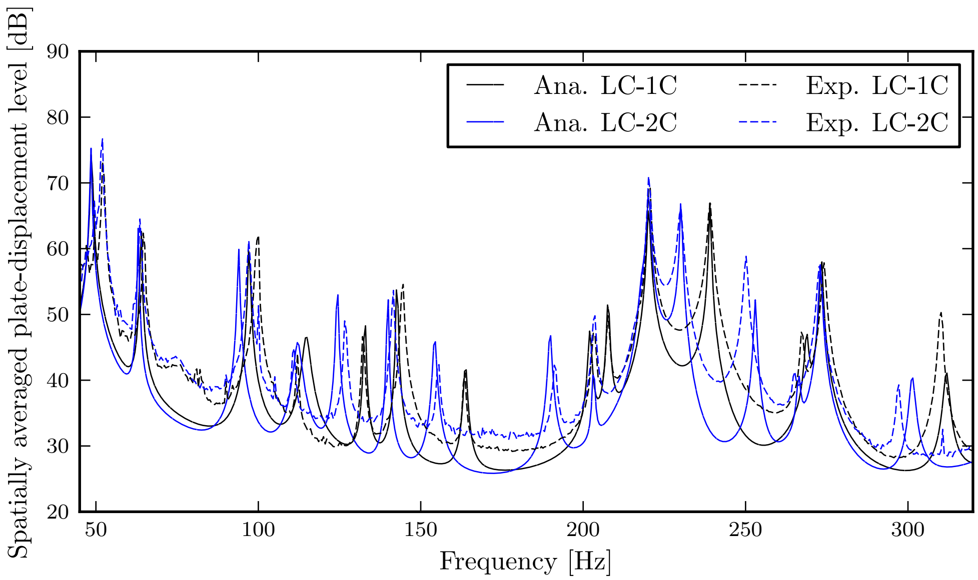

Figure 10: RMS plate-displacement level spectrum for LC-1C and LC-2C.

5.3 MAC analysis

In order to compare the experimental and analytical mode shapes quantitatively, a MAC analysis was employed for all the load cases. The MAC results are presented in Fig. 13-16. The numbers close to 1 on the diagonals show that the similarity between the analytical and experimental mode shapes is very good. In some cases a cluster of high values can be observed on the diagonal. This means that for the corresponding peaks the plate vibrates with almost identical mode shapes.

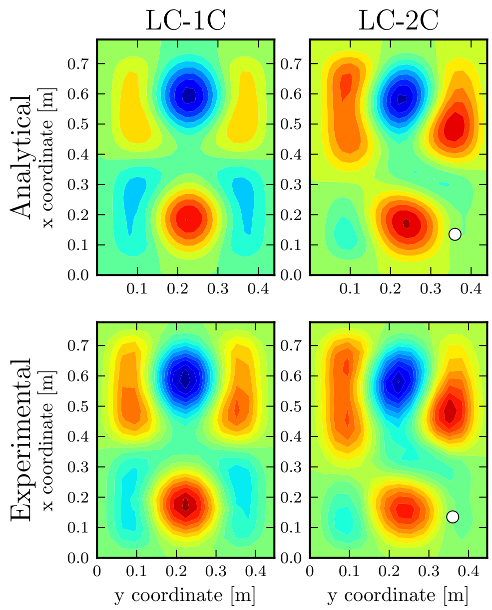

Figure 11: Comparison of the clamped plate mode shapes at first cavity controlled mode at approximately 220 Hz. The symbol '∘' represents the mass location.

5.4 Overview of the results

From the presented results it can be determined that the implemented structural-acoustic model provides good predictions of acoustic and plate levels, compared to the measurements. Furthermore, changes in coupled-system response due to added mass are also accurately predicted. This also indicates that experimental setup correctly replicated assumed plate boundary conditions and that a loudspeaker can be successfully represented by using a group of point sources.

To summarize the structural-acoustic behaviour of the coupled system, the cavity pressures, seen on Figures 9 and 12, are controlled mainly by the acoustic modes, while the plate deflection, seen on Figures 7 and 10, is controlled by the structural modes and above second acoustic mode (see Table 6) also by acoustic modes. From Table 8 it can be seen that added mass weakly affects structural modes frequency wise; however, the plate mode shapes can be significantly affected as can be seen in figures 8 and 11.

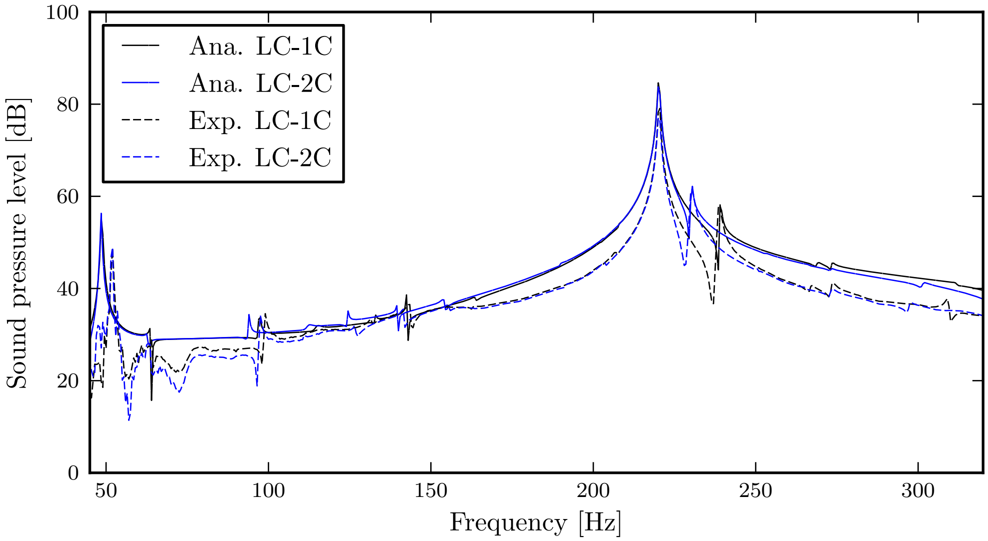

Figure 12: Amplitude spectrum of sound-pressure level for LC-1C and LC-2C.

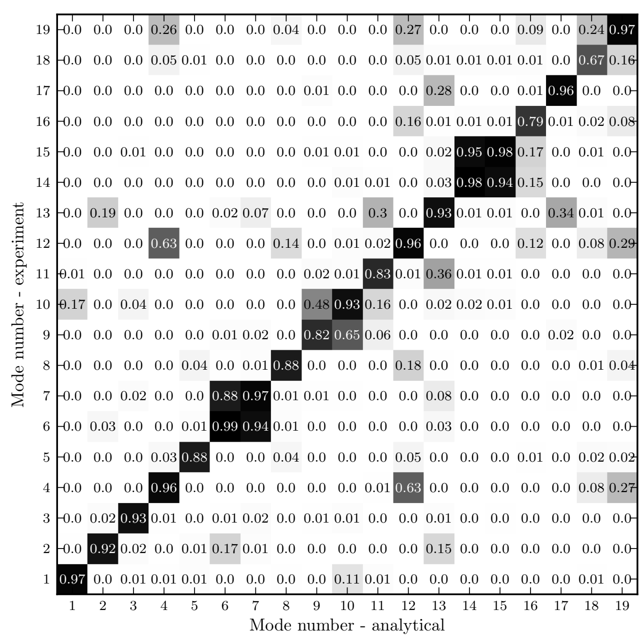

Figure 13: Modal assurance criterion results for LC-1S.

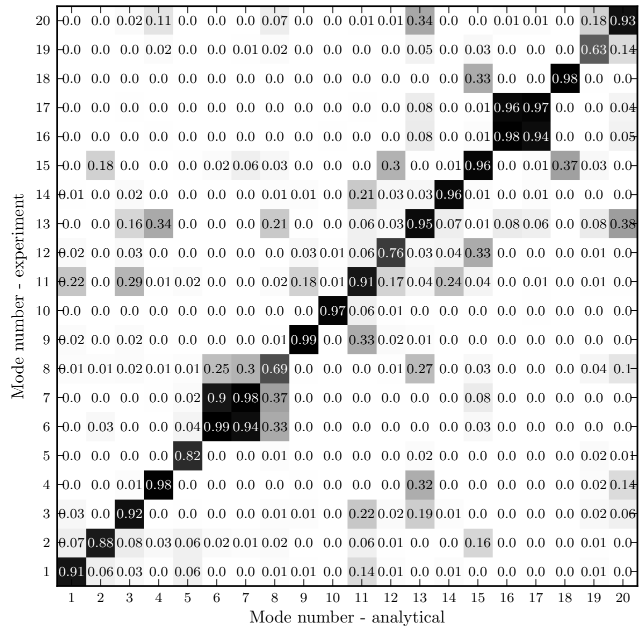

Figure 14: Modal assurance criterion results for LC-2S.

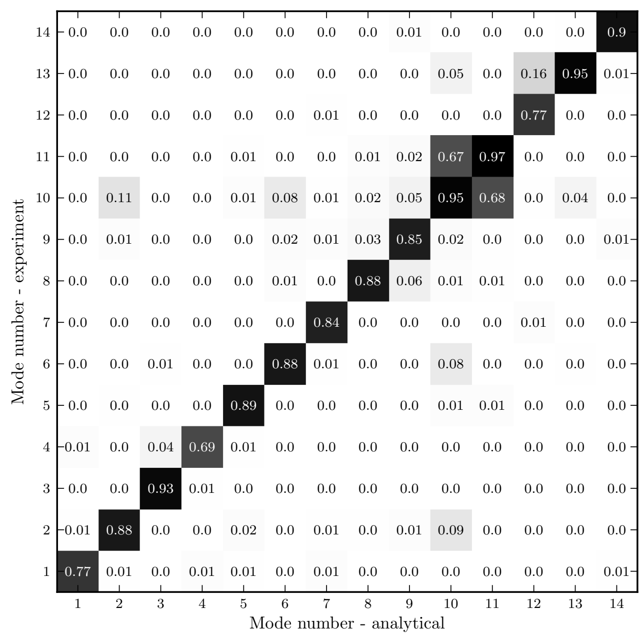

Figure 15: Modal assurance criterion results for LC-1C.

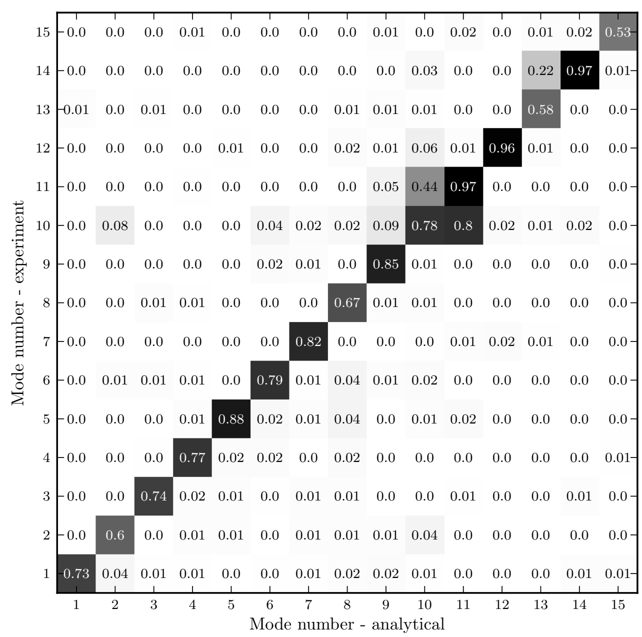

Figure 16: Modal assurance criterion results for LC-2C.

6 Conclusion

A structural-acoustic model of a plate-cavity system with an attached distributed mass and internal sound source was developed by combining three approaches. The first approach is based on a recently presented analysis with the Rayleigh-Ritz method [14], which provided the uncoupled plate mode shapes needed in the second approach, i.e., the modal-interaction approach. This was necessary due to the unavailability of the analytical expressions for a plate loaded with a distributed mass. Furthermore, it facilitates the use of various plate boundary conditions and the arbitrary size and location of the attached distributed mass. The appropriate approximation functions and the selection process of the key parameters were shown. The system was excited by an internal sound source, which in the third approach is represented by a group of point sources generating an acoustic pulse in the time domain.

The structural-acoustic model was validated by conducting an experiment. A plexiglass box was coupled with two different aluminium plates in simply-supported and clamped configurations. The system was excited by an acoustic pulse from a loudspeaker in the interior of the plexiglass box. The acoustic and structural response was measured and compared to the results from a computer implementation of the structural-acoustic model. The results were compared for four different load cases and good agreement was found. From the results it can also be concluded that the loudspeaker used in experiment was correctly represented by the group of point sources.

Acknowledgement

Operation part financed by the European Union, European Social Fund.

References

[1] F. Fahy, P. Gardonio, Sound and structural vibration: radiation, transmission and response, Academic Press, Elsevier/Academic, 2007.

[2] E. Dowell, H. Voss, The effect of a cavity on panel vibration, AIAA Journal 1 (1963) 476–477.

[3] R. H. Lyon, Noise reduction of rectangular enclosures with one flexible wall, The Journal of the Acoustical Society of America 35 (11) (1963) 1791–1797.

[4] E. Dowell, G. Gorman, D. Smith, Acoustoelasticity: general theory, acoustic natural modes and forced response to sinusoidal excitation, including comparisons with experiment, Journal of Sound and Vibration 52 (4) (1977) 519–542.

[5] M. Al-Bassyiouni, B. Balachandran, Sound transmission through a flexible panel into an enclosure: structural-acoustics model, Journal of Sound and Vibration 284 (1-2) (2005) 467–486.

[6] A. Blevins, Formulas for natural frequency and mode shapes, Krieger, 1979.

[7] J.-B. Dupont, M.-A. Galland, Active absorption to reduce the noise transmitted out of an enclosure, Applied Acoustics 70 (1) (2009) 142–152.

[8] B. Venkatesham, M. Tiwari, M. L. Munjal, Analytical prediction of break-out noise from a reactive rectangular plenum with four flexible walls, Journal of the Acoustical Society of America 128 (4, Part 1) (2010) 1789–1799.

[9] S. Y. Park, S. H. Kim, Y. J. Kang, The effect of a local stiffener in the structural-acoustic coupled system, Proceedings of the Institution of Mechanical Engineers Part C-Journal of Mechanical Engineering Science 224 (C9) (2010) 1915–1931.

[10] Y. Yoon, J. Lee, S. Yoo, H. Choi, A new method for in-plane vibration analysis of circular rings with widely distributed deviation, Journal of Sound and Vibration 254 (4) (2002) 787–800.

[11] R. Stpierre, G. Koopman, A design method for minimizing the sound power radiated from plates by adding optimally sized, discrete masses, Journal of Mechanical Design 117 (B) (1995) 243–251.

[12] E. Constans, G. Koopmann, A. Belegundu, The use of modal tailoring to minimize the radiated sound power of vibrating shells: theory and experiment, Journal of Sound and Vibration 217 (2) (1998) 335–350.

[13] S. Li, X. Li, The effects of distributed masses on acoustic radiation behavior of plates, Applied Acoustics 69 (3) (2008) 272–279.

[14] W. Wong, The effects of distributed mass loading on plate vibration behavior, Journal of Sound and Vibration 252 (3) (2002) 577–583.

[15] C. G. Boay, Frequency analysis of rectangular isotropic plates carrying a concentrated mass, Computers & Structures 56 (1) (1995) 39 – 48.

[16] M. Richardson, Is it a mode shape, or an operating deflection shape?, Sound And Vibration 31 (1) (1997) 54–61.

[17] N. M. M. Maia, J. M. M. Silva, J. He, N. A. J. Lieven, R. M. Lin, G. W. Skingle, W. To, A. P. V. Urgueira, Theoretical and experimental modal analysis, Mechanical Engineering Research Studies: Engineering Dynamics Series, Taylor & Francis, 1997.